Imaging of domain-inverted gratings in $LiNbO_3$ by electrostatic force microscopy

H. Bluhm,[a] A. Wadas, and R. Wiesendanger
Institute of Applied Physics and Microstructure Research Center, University of Hamburg, D-20355 Hamburg, Germany

A. Roshko[b] and J. A. Aust
National Institute of Standards and Technology, Boulder, Colorado 80303

D. Nam
SDL Inc., San Jose, California 95134

(Received 6 February 1997; accepted for publication 30 April 1997)

Ferroelectric domains in $LiNbO_3$ have been investigated by means of electrostatic force microscopy. Polarization-inverted gratings with 4 μm periodicity were fabricated by titanium diffusion into both $+c$ and $-c$ faces of single-domain $LiNbO_3$ crystals. The distribution of the electric field in the vicinity of the sample surface was measured using scanning probe microscopy. The electrostatic force image was found to correlate with the shape of the domain-inverted profile observed by scanning electron and optical microscopies. © *1997 American Institute of Physics.* [S0003-6951(97)01927-X]

Domain-inverted gratings have the potential for a wide range of optical device applications including second-harmonic generators, sum–frequency generators, and optical parametric oscillators. However, control of the domain shape remains an obstacle. This problem is aggravated by the lack of a nondestructive, high-resolution technique for imaging ferroelectric domains. Scanning electron microscopy (SEM),[1] transmission electron microscopy,[2] and optical microscopy[3] have been used to image ferroelectric domains in $LiNbO_3$ crystals. Recently, it has been demonstrated that electrostatic force microscopy (EFM) is able to map the domain structure of ferroelectric crystals with 50 nm lateral resolution.[4–6] In comparison with other techniques, EFM is nondestructive and has the advantage that the magnitude and distribution of the electric field in the vicinity of the sample surface can be imaged. We present here the results of EFM investigations of periodically poled structures fabricated in $LiNbO_3$ crystals.

EFM images were obtained in the dc mode using a commercially available scanning probe microscope. Measurements were carried out in two steps in order to monitor the topography and the electrostatic force separately from each other. First, the tip tracked one scan line in contact with the sample to determine the surface topography. Then, the tip was raised to a predetermined height (from 50 to 100 nm) above the surface and scanned parallel to the previously stored scan line.[7] Based on the topography measured with the contact scan, the tip–sample separation was kept constant during the noncontact scan. The deflection of the cantilever due to the electrostatic force from the sample was then plotted as a function of position during the noncontact scan. For the (EFM) measurements, commercially available Si cantilevers with spring constants of 4 N/m were used.

Polarization-inverted gratings were produced by Ti diffusion into both $+c$ (the $+c$ sample) and $-c$ (the $-c$ sample) faces of single domain $LiNbO_3$ crystals.[8] In the Ti diffused regions, the direction of the macroscopic polarization is inverted relative to that of the rest of the crystal. For both samples, the grating periodicity was 4 μm. For the $+c$ sample, the Ti was diffused from 5 nm thick, 2 μm wide parallel stripes separated by 2 μm, into the $+c$ face. For the $-c$ sample, the Ti was diffused from 5 nm thick, 0.7 μm wide stripes separated by 3.3 μm, into the $-c$ face. After electric-field imaging, a y face of each sample was polished, then etched[9] to make the domain-inverted regions visible by SEM and optical microscopy.

Cross sections of the domain-inverted regions are shown in Fig. 1. Figure 1(a) is a SEM image of the domain profile

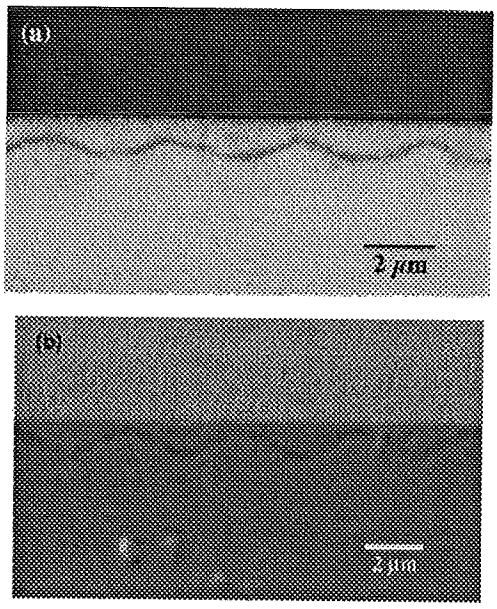

FIG. 1. (a) SEM micrograph of the domain-inverted profile cross section in the $+c$ sample (diffused from the $+c$ face), and (b) optical micrograph of the domain-inverted profile cross section in the $-c$ sample (diffused from the $-c$ face). Both gratings have a periodicity of 4 μm.

[a]Present address: Lawrence Berkeley National Laboratory, Materials Science Division (Bldg. 66), 1 Cyclotron Road Berkeley, CA 94720.
[b]Electronic mail: roshko@boulder.nist.gov

 0003-6951/97/71(1)/146/3/$10.00 © 1997 American Institute of Physics

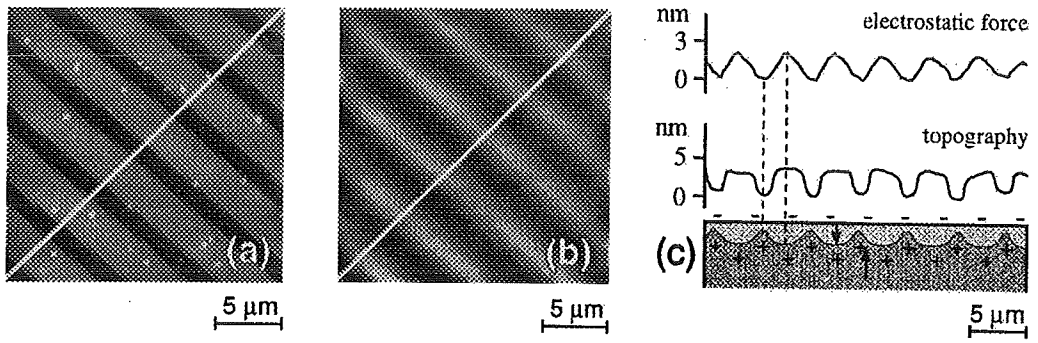

FIG. 2. EFM measurements of the $+c$ face of the $+c$ sample. The scan size is 20 μm×20 μm. (a) A topographic image. The higher (brighter) areas are the Ti-diffused regions. (b) The electrostatic signal from the same area shown in (a). Darker regions indicates a stronger attractive force. (c) Cross sections of the electrostatic (top) and topography (center) signals taken at the lines indicated in (a) and (b), and a schematic drawing of the domain profile observed by SEM (bottom). The arrows mark the direction of the spontaneous polarization in the respective sample regions. The boundary between the domain-inverted (brighter regions) and uninvested regions of the sample carries a positive charge.

resulting from Ti diffusion in the $+c$ sample. An optical image of the domain profile in the $-c$ sample is shown in Fig. 1(b). The dark line of contrast in both images is the interface between the inverted and uninverted polarization regions. As expected, the gratings have a periodicity of 4 μm. In both samples, the surface is polarization-inverted relative to the bulk.

Figure 2(a) shows the topography of the $+c$ face of the $+c$ sample as observed during EFM. Since the Ti diffusion causes the lattice to swell,[10] the diffused regions (~3 μm wide) are raised above the rest of the surface. Figure 2(b) is an image of the electrostatic force acting on the cantilever measured over the same area imaged in Fig. 2(a). Here, the darker regions indicate a stronger attractive force on the tip. The maximum deflection of the cantilever was 2 nm, corresponding to a force of 8×10^{-9} N. The electrostatic contrast has the same periodicity as the topography of the sample.

Figure 2(c) shows cross sections taken along the lines, which are indicated in Figs. 2(a) and 2(b). The domain profile as determined by SEM is sketched in the lower part of Fig. 2(c) in relation to the surface topography and the electrostatic signal. Comparison of the domain profile and the electrostatic contrast reveals a depression in the electrostatic force signal above the 1 μm wide regions where less material has been inverted. At these points, there is the strongest attraction between the field from the sample and the tip.

The observed electrostatic contrast can be explained by the presence of a permanent negative charge in the Si tip,[11,12] which interacts with the electric field above the surface of the sample. The magnitude and distribution of this field appear to be determined by the shape of the domain-inverted regions. Below the domain-inverted region, the crystal is polarized with the positive charge toward the surface. The field produced by this polarization is modified by the opposing polarization of the domain-inverted regions at the surface. In regions where little material is inverted, the field from the underlying material is strong, and the negatively charged tip is attracted to the sample surface. In regions where more material has been inverted, the opposing field is larger and the tip–sample interaction is weaker or may even be repulsive. Therefore, the tip moves away from the sample above these regions.

EFM measurements of the $-c$ face of the $-c$ sample are presented in Fig. 3. The topography image is shown in Fig. 3(a). Again, the periodicity of the grating (4 μm) is in agreement with the optical observations [see Fig. 1(b)]. The simultaneously measured electrostatic force on the cantilever is shown in Fig. 3(b). Again, the electrostatic contrast exhibits the same periodicity as the domain-inverted grating. Cross sections of the electrostatic force signal and the topography taken along the lines indicated in Figs. 3(a) and 3(b) are shown in Fig. 3(c). In the bottom part of Fig. 3(c), a schematic drawing of the domain profile of the $-c$ sample is shown [cf. Fig. 1(b)] in relation to the topography and the electrostatic signals.

In this sample, a positive deflection is observed in the

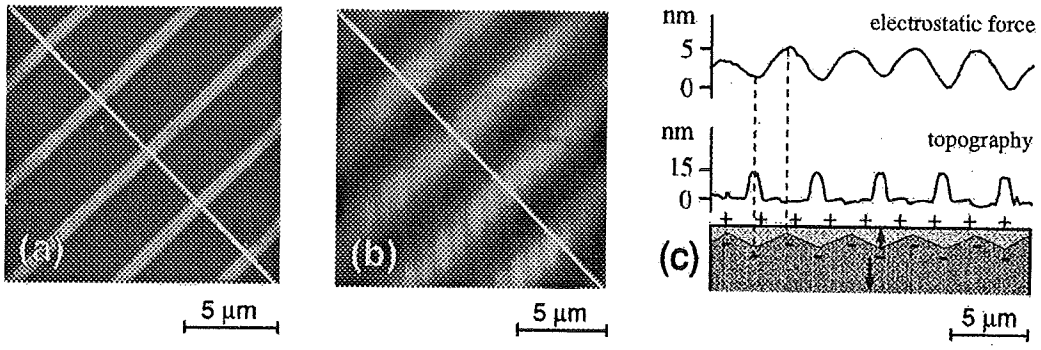

FIG. 3. EFM measurements of the $-c$ face of the $-c$ sample. The scan size is 15 μm×15 μm. (a) A topographic image of the grating. (b) The electrostatic force observed at the same area shown in (a). Cross sections of the electrostatic (top) and topography (center) signals taken at the lines indicated in (a) and (b) and a schematic drawing of the domain profile (bottom). The interface between the inverted and uninvested parts of the sample carries a negative charge.

electrostatic force signal above the 3 μm wide regions where less material has been domain inverted. In the $+c$ sample, the shape of the electrostatic force signal, the surface-topography, and the domain profile are all similar. However, in the $-c$ sample, the electrostatic force signal is quite different from the surface topography and more closely resembles the domain profile [as shown in Fig. 3(c)].

As for the $+c$ sample, the electrostatic contrast in the $-c$ sample can be explained by the interaction of a negatively charged tip with the electric field, which arises from the domain-inversion profile. In this case, the bulk of the crystal is polarized with a negative charge toward the surface. Therefore, in regions where little material has been inverted at the surface, the tip is strongly repelled by the sample. In regions where diffusion has caused more material to invert, the repulsion is less, and the tip relaxes back toward the sample, corresponding to depressions in the electrostatic force image.

In summary, we have imaged the electric field, which arises from a periodically poled structure in $LiNbO_3$ crystals by means of EFM. The contrast in the electrostatic image has been explained by the interaction of a permanent negative charge in the tip with the field above the sample surface. This field results from both the bulk sample polarization and the modifying polarization of the domain-inverted regions at the surface. Due to its sensitivity, EFM is capable of resolving changes in the electric-field distribution just above the surface of the $LiNbO_3$ surface on a submicrometer scale.

[1] D. V. Roshchupkin, M. Brunel, R. Tucoulou, E. Bigler, and N. G. Sorokin, Appl. Phys. Lett. **64**, 164 (1994).
[2] V. A. Meleshina, N. V. Belugina, E. V. Rakova, Kh. S. Bagdasarov, N. D. Zakharov, and V. N. Rozhanskii, Sov. Phys. Crystallogr. **29**, 680 (1984).
[3] A. I. Otko, A. E. Nosenko, T. R. Volk, and L. A. Shuvalov, Ferroelectrics **145**, 163 (1993).
[4] F. Saurenbach and B. D. Terris, Appl. Phys. Lett. **56**, 1703 (1990).
[5] R. Lüthi, H. Haefke, K.-P. Meyer, E. Meyer, L. Howald, and H.-J. Güntherodt, J. Appl. Phys. **74**, 7461 (1993).
[6] T. Hidaka, T. Maruyama, M. Saitoh, N. Mikoshiba, M. Shimizu, T. Shiosaki, L. A. Wills, R. Hiskes, S. A. Dicarolis, and J. Amano, Appl. Phys. Lett. **68**, 2358 (1996).
[7] K. Babcock, M. Dugas, S. Manalis, and V. Elings, Mater. Res. Soc. Symp. Proc. **355**, 311 (1995).
[8] S. Thaniyavarn, T. Findakly, D. Booher, and J. Moen, Appl. Phys. Lett. **46**, 933 (1985).
[9] K. Nassau, H. J. Levinstein, and G. M. Loiacono, J. Phys. Chem. Solids **27**, 983 (1966).
[10] G. J. Griffiths and R. J. Esdaile, IEEE J. Quantum Electron. **QE-20**, 149 (1984).
[11] H.-J. Butt, Nanotechnology **3**, 60 (1992).
[12] H. Bluhm, A. Wadas, R. Wiesendanger, K.-P. Meyer, and L. Szczesniak, Phys. Rev. B **55**, 4 (1997).